HAL
open science

Creation of a Transport Barrier for the E x B drift in magnetized plasmas

Michel Vittot, Natalia Tronko

To cite this version:

Michel Vittot, Natalia Tronko. Creation of a Transport Barrier for the E x B drift in magnetized plasmas. Annals of the University of Craiova Physics AUC , 2009, 19, pp.59-72. hal-00477163

HAL Id: hal-00477163

https://hal.science/hal-00477163v1

Submitted on 28 Apr 2010

HAL is a multi-disciplinary open access archive for the deposit and dissemination of scientific research documents, whether they are published or not. The documents may come from teaching and research institutions in France or abroad, or from public or private research centers.

L'archive ouverte pluridisciplinaire **HAL**, est destinée au dépôt et à la diffusion de documents scientifiques de niveau recherche, publiés ou non, émanant des établissements d'enseignement et de recherche français ou étrangers, des laboratoires publics ou privés.

Physics AUC, vol. 19, 59-72 (2009)

Creation of a Transport Barrier for the $E \times B$ drift in magnetized plasmas

Natalia Tronko, Michel Vittot

Centre de Physique Théorique (CPT) - CNRS, Luminy - Case 907,

13288 Marseille cedex 09, France.

Unité Mixte de Recherche (UMR 6207) du CNRS, et des universités

Aix-Marseille I, Aix-Marseille II et du Sud Toulon-Var.

Laboratoire affilié à la FRUMAM (FR 2291).

Laboratoire de Recherche Conventionné du CEA (DSM-06-35).

E-mail: Nathalie.Tronko@cpt.univ-mrs.fr, Michel.Vittot@cpt.univ-mrs.fr

Abstract

We modelize the chaotic dynamics of charged test-particles in a turbulent electric field, across the confining magnetic field in controlled thermonuclear fusion devices by a $1\frac{1}{2}$ degrees of freedom Hamiltonian dynamical system. The external electric field $\mathbf{E} = -\nabla V$ is given by a some potential V and the magnetic field $\mathbf{B}$ is considered uniform. We prove that, by introducing a small additive control term to the external electric field, it is possible to create a transport barrier. The robustness of this control method is also numerically investigated.

1 Introduction

The confinement properties of high performance plasmas with magnetic confinement are governed by electromagnetic turbulence that develops in microscales [1]. In that framework various scenarios are explored to lower the turbulent transport and therefore improve the overall performance of a given device. The aim of such a research activity is two-fold.

In this paper, we propose an alternative approach to transport barriers based on a macroscopic control of the $E \times B$ turbulence. Our theoretical study is based on a localized hamiltonian control method that is well suited for $E \times B$ transport. In a previous approach [3], a more global scheme was proposed with a reduction of turbulent transport at each point of the phase space. In the present work, we derive an exact expression to govern a local control at a chosen position in phase space. In principle, such an approach allows one to generate the required transport barriers in the regions of interest without enforcing large modification of the confinement properties to achieve an ITB formation [2]. Although the application of such a precise control scheme remains to be assessed, our approach shows that local control transport barriers can be generated without requiring macroscopic changes of the plasma properties to trigger such barriers. The scope of the present work is the theoretical demonstration of the control scheme and consequently the possibility of generating transport barriers based on more specific control schemes than envisaged in present advanced scenarios.

Talk given at International Workshop "Anomalous Transport in Fusion Plasmas", October 6-8, 2008, Craiova, Romania

In Section 2, we give the general description of our model and the physical motivations for our investigation. In Section 4, we explain the general method of *localized control* for Hamiltonian systems and we estimate the size of the control term. Section 5 is devoted to the numerical investigations of the control term, and we discuss its robustness and its energy cost. The last section 6 is devoted to conclusions and discussion.

2 Physical motivations and the $E \times B$ model

2.1 Physical motivations

Fusion plasma are sophisticated systems that combine the intrinsic complexity of neutral fluid turbulence and the self-consistent response of charged species, both electrons and ions, to magnetic fields. Regarding magnetic confinement in a tokamak, a large external magnetic field and a first order induced magnetic field are organised to generate the so-called magnetic equilibrium of nested toroidal magnetic surfaces [4]. Experimental strategies in advanced scenarios comprising Internal Transport Barriers are based on means to enforce these two control schemes. In both cases they aim at modifying macroscopically the discharge conditions to fulfill locally the Chirikov criterion. It thus appears interesting to devise a control scheme based on a less intrusive action that would allow one to modify the chaotic transport locally by the choice of an appropriate electrostatic perturbation hence leading to a local transport barrier.

3 The $E \times B$ model

For fusion plasmas, the magnetic field B is slowly variable with respect to the inverse of the Larmor radius ρ_L i.e: $\rho_L |\nabla \ln B| \ll 1$. This fact allows the separation of the motion of a charged test particle into a slow motion (parallel to the lines of the magnetic field) and a fast motion (Larmor rotation). This fast motion is named gyromotion, around some gyrocenter. In first approximation the averaging of the gyromotion over the gyroangle gives the approximate trajectory of the charged particle. This averaging is the guiding-center approximation.

In this approximation, the equations of motion of a charged test particle in the presence of a strong uniform magnetic field $\mathbf{B} = B\hat{\mathsf{z}}$, (where $\hat{\mathsf{z}}$ is the unit vector in the z direction) and of an external time-dependent electric field $\mathbf{E} = -\boldsymbol{\nabla} V_1$ are:

$$\begin{aligned} \frac{d}{dT}\begin{pmatrix} X \\ \\ Y \end{pmatrix} &= \frac{c\mathbf{E}\times\mathbf{B}}{B^2} = \frac{c}{B}\,\mathbf{E}(X,Y,T)\times\hat{\mathsf{z}} \\ &= \frac{c}{B}\begin{pmatrix} -\partial_Y V_1(X,Y,T) \\ \\ \partial_X V_1(X,Y,T) \end{pmatrix} \end{aligned} \tag{1}$$

where V_1 is the electric potential. The spatial coordinates X and Y play the role of canonically-conjugate variables and the electric potential $V_1(X,Y,T)$ is the Hamiltonian for the problem. Now the problem is placed into a parallelepipedic box with dimensions $L \times \ell \times (2\pi/\omega)$, where L and ℓ are some characteristic lengths and ω is a characteristic frequency of our problem, X is locally a radial coordinate and Y is a poloidal coordinate.

A phenomenological model [5] is chosen for the potential:

$$V_1(X,Y,T) = \sum_{n,m=1}^{N} \frac{V_0 \ \cos\chi_{n,m}}{(n^2+m^2)^{3/2}} \tag{2}$$

where V_0 is some amplitude of the potential,

$$\chi_{n,m} \equiv \frac{2\pi}{L} nX + \frac{2\pi}{\ell} mY + \phi_{n,m} - \omega T$$

ω is constant, for simplifying the numerical simulations and $\phi_{n,m}$ are some random phases (uniformly distributed).

We introduce the dimensionless variables

$$(x,y,t) \equiv (2\pi X/L,\ 2\pi Y/\ell,\ \omega T) \tag{3}$$

So the equations of motion (1) in these variables are:

$$\frac{d}{dt}\begin{pmatrix} x \\ y \end{pmatrix} = \begin{pmatrix} -\partial_y V(x,y,t) \\ \partial_x V(x,y,t) \end{pmatrix} \tag{4}$$

where $V = \varepsilon(V_1/V_0)$ is a dimensionless electric potential given by

$$V(x,y,t) = \varepsilon \sum_{n,m=1}^{N} \frac{\cos\left(nx + my + \phi_{n,m} - t\right)}{(n^2+m^2)^{3/2}} \tag{5}$$

Here

$$\varepsilon = 4\pi^2 (cV_0/B)/(L\ell\omega) \tag{6}$$

is the small dimensionless parameter of our problem. We perturb the model potential (5) in order to build a transport barrier. The system modeled by Eqs.(4) is a $1\frac{1}{2}$ degrees of freedom system with a chaotic dynamics [5, 3]. The poloidal section of our modeled tokamak is a Poincaré section for this problem and the stroboscopic period will be chosen to be 2π, in term of the dimensionless variable t.

The particular choice (2) or (5) is not crucial and can be generalized. Generally, ω can be chosen depending on n, m. This would make the numerical computations more involved. In the following section, V is chosen completely arbitrary.

4 Localized control theory of hamiltonian systems

4.1 The control term

In this section we show how to construct a transport barrier for any electric potential V. The electric potential $V(x,y,t)$ yields a non-autonomous Hamiltonian. We expand the two-dimensional phase space by including the canonically-conjugate variables (E,τ),

$$H = H(E,x,y,\tau) = E + V(x,y,\tau) \tag{7}$$

The Hamiltonian of our system thus becomes autonomous. Here τ is a new variable whose dynamics is trivial: $\dot{\tau} = 1$ i.e. $\tau = \tau_0 + t$ and E is the variable canonically conjugate to τ.

The Poisson bracket in the expanded phase space for any $W = W(E, x, y, \tau)$ is given by the expression:

$$\{W\} \equiv (\partial_x W)\partial_y - (\partial_y W)\partial_x + (\partial_E W)\partial_\tau - (\partial_\tau W)\partial_E. \tag{8}$$

Hence $\{W\}$ is a linear (differential) operator acting on functions of (E, x, y, τ). We call $H_0 = E$ the unperturbed Hamiltonian and $V(x, y, \tau)$ its perturbation. We now implement a perturbation theory for H_0. The bracket (8) for the Hamiltonian H is

$$\{H\} = (\partial_x V)\partial_y - (\partial_y V)\partial_x + \partial_\tau - (\partial_\tau V)\partial_E \tag{9}$$

So the equations of motion in the expanded phase space are:

$$\dot{y} = \{H\}y = \partial_x V(x, y, \tau) \tag{10}$$
$$\dot{x} = \{H\}x = -\,\partial_y V(x, y, \tau) \tag{11}$$
$$\dot{E} = \{H\}E = -\,\partial_\tau V(x, y, \tau) \tag{12}$$
$$\dot{\tau} = \{H\}\tau = 1 \tag{13}$$

We want to construct a small modification F of the potential V such that

$$\widetilde{H} \equiv E + V(x, y, \tau) + F(x, y, \tau) \equiv E + \widetilde{V}(x, y, \tau) \tag{14}$$

has a barrier at some chosen position $x = x_0$. So the control term

$$F = \widetilde{V}(x, y, \tau) - V(x, y, \tau) \tag{15}$$

must be much smaller than the perturbation (e.g., quadratic in V). One of the possibilities is:

$$\widetilde{V} \equiv V(x + \partial_y f(y, \tau), y, \tau) \tag{16}$$

where

$$f(y, \tau) \equiv \int_0^\tau V(x_0, y, t)dt$$

Indeed we have the following theorem:

Theorem 1 *The Hamiltonian $\widetilde{H}$ has a trajectory $x = x_0 + \partial_y f(y, \tau)$ acting as a barrier in phase space.*

Proof

Let the Hamiltonian $\widehat{H} \equiv \exp(\{f\})\tilde{H}$ be canonically related to $\widetilde{H}$. (Indeed the exponential of any Poisson bracket is a canonical transformation.) We show that $\widehat{H}$ has a simple barrier at $x = x_0$. We start with the computation of the bracket (8) for the function f. Since $f = f(y, \tau)$, the expression for this bracket contains only two terms,

$$\{f\} \;\equiv\; -f'\partial_x \;-\; \dot{f}\partial_E \tag{17}$$

where

$$f' \equiv \partial_y f \text{ and } \dot{f} \equiv \partial_\tau f \tag{18}$$

which commute:

$$[f'\partial_x, \dot{f}\partial_E] = 0 \tag{19}$$

Now let us compute the coordinate transformation generated by $\exp(\{f\})$:

$$\exp(\{f\}) \;\equiv\; \exp(-f'\partial_x)\;\exp(-\dot{f}\partial_E), \tag{20}$$

where we used (19) to separate the two exponentials.

Using the fact that $\exp(b\partial_x)$ is the translation operator of the variable x by the quantity b: $[\exp(b\partial_x)W](x) = W(x+b)$, we obtain

$$\begin{aligned}
\widehat{H} = e^{\{f\}}\tilde{H} \;&\equiv\; e^{\{f\}}E \;+\; e^{\{f\}}\tilde{V}(x,y,\tau) \\
&= \left(E \;-\; \dot{f}\right) \;+\; \widetilde{V}\,(x-f',y,\tau) \\
&= E \;-\; V(x_0,y,\tau) \;+\; V(x+f'-f',y,\tau) \\
&= E - V(x_0,y,\tau) + V(x,y,\tau)
\end{aligned} \tag{21}$$

This Hamiltonian has a simple trajectory $x = x_0, E = E_0$, i.e. any initial data $x = x_0,\; y = y_0, E = E_0, \tau = \tau_0$ evolves under the flow of $\widehat{H}$ into $x = x_0, y = y_t, E = E_0, \tau = \tau_0 + t$ for some evolution y_t that may be complicated, but not useful for our problem. Hamilton's equations for x and E are now

$$\dot{x} = \{\widehat{H}\}x = \partial_y\left[V(x_0,y,\tau) - V(x,y,\tau)\right] \tag{22}$$

$$\dot{E} = \{\widehat{H}\}E = \partial_\tau\left[V(x_0,y,\tau) - V(x,y,\tau)\right] \tag{23}$$

so that for $x = x_0$, we find $\dot{x} = 0 = \dot{E}$. Then the union of all points (x,y,E,τ) at $x = x_0 \;\; E = E_0$:

$$\mathfrak{B}_0 = \bigcup_{y,\tau,E_0} \begin{pmatrix} x_0 \\ y \\ E_0 \\ \tau \end{pmatrix} \tag{24}$$

is a 3-dimensional surface $\mathbb{T}^2 \times \mathbb{R}$, ($\mathbb{T} \equiv \mathbb{R}/2\pi\mathbb{Z}$) preserved by the flow of $\widehat{H}$ in the 4-dimensional phase space. If an initial condition starts on $\mathfrak{B}_0$, its evolution under the flow $\exp(t\{\hat{H}\})$ will remain on $\mathfrak{B}_0$.

So we can say that $\mathfrak{B}_0$ act as a barrier for the Hamiltonian $\widehat{H}$: the initial conditions starting inside $\mathfrak{B}_0$ can't evolve outside $\mathfrak{B}_0$ and vice-versa.

To obtain the expression for a barrier $\mathfrak{B}$ for $\widetilde{H}$ we deform the barrier for $\widehat{H}$ via the transformation $\exp(\{f\})$. As

$$\widetilde{H} = e^{-\{f\}}\widehat{H} \tag{25}$$

and $\exp(\{f\})$ is a canonical transformation, we have

$$\{\widetilde{H}\} = \{e^{-\{f\}}\widehat{H}\} = e^{-\{f\}}\{\widehat{H}\}e^{\{f\}} \tag{26}$$

Now let us calculate the flow of $\widetilde{H}$:

$$e^{t\{\widetilde{H}\}} = e^{t\left(e^{-\{f\}}\{\widehat{H}\}e^{\{f\}}\right)} = e^{-\{f\}}e^{t\{\widehat{H}\}}e^{\{f\}} \tag{27}$$

Indeed:

$$e^{t\left(e^{-\{f\}}\{\widehat{H}\}e^{\{f\}}\right)} = \sum_{n=0}^{\infty} \frac{t^n(e^{-\{f\}}\{\widehat{H}\}e^{\{f\}})^n}{n!} \tag{28}$$

For instance when $n = 2$:

$$t^2(e^{-\{f\}}\{\widehat{H}\}e^{\{f\}})^2 = t^2 e^{-\{f\}}\{\widehat{H}\}e^{\{f\}}e^{-\{f\}}\{\widehat{H}\}e^{\{f\}}$$

$$= t^2 e^{-\{f\}} \{\widehat{H}\}^2 e^{\{f\}} \tag{29}$$

and so

$$e^{t\{\widetilde{H}\}} = \sum_{n=0}^{\infty} \frac{t^n e^{-\{f\}} \{\widehat{H}\}^n e^{\{f\}}}{n!} = e^{-\{f\}} e^{t\{\widehat{H}\}} e^{\{f\}} \tag{30}$$

As we have seen before:

$$e^{\{f\}} \begin{pmatrix} x \\ y \\ E \\ \tau \end{pmatrix} = \begin{pmatrix} x - f' \\ y \\ E - \dot{f} \\ \tau \end{pmatrix}$$

and

$$e^{t\{\widehat{H}\}} \begin{pmatrix} x_0 \\ y \\ E_0 \\ \tau \end{pmatrix} = \begin{pmatrix} x_0 \\ y_t \\ E_0 \\ \tau + t \end{pmatrix} \tag{31}$$

Multiplying (27) on the right by $e^{-\{f\}}$ we obtain:

$$e^{t\{\widetilde{H}\}} e^{-\{f\}} = e^{-\{f\}} e^{t\{\widehat{H}\}}$$

$$e^{t\{\widetilde{H}\}} e^{-\{f\}} \begin{pmatrix} x_0 \\ y \\ E_0 \\ \tau \end{pmatrix} = e^{t\{\widetilde{H}\}} \begin{pmatrix} x_0 + f'(y,\tau) \\ y \\ E_0 + \dot{f}(y,\tau) \\ \tau \end{pmatrix} \tag{32}$$

and

$$e^{-\{f\}} e^{t\{\widehat{H}\}} \begin{pmatrix} x_0 \\ y \\ E_0 \\ \tau \end{pmatrix} = e^{-\{f\}} \begin{pmatrix} x_0 \\ y_t \\ E_0 \\ \tau + t \end{pmatrix}$$

$$= \begin{pmatrix} x_0 + f'(y_t, \tau + t) \\ y_t \\ E_0 + \dot{f}(y_t, \tau + t) \\ \tau + t \end{pmatrix} \tag{33}$$

So the flow $\exp(t\{\widetilde{H}\})$ preserves the set

$$\mathfrak{B} = \bigcup_{y,\tau,E_0} \begin{pmatrix} x_0 + f'(y,\tau) \\ y \\ E_0 + \dot{f}(y,\tau) \\ \tau \end{pmatrix} \tag{34}$$

$\mathfrak{B}$ is a 3 dimensional invariant surface, topologically equivalent to $\mathbb{T}^2 \times \mathbb{R}$ into the 4 dimensional phase space. $\mathfrak{B}$ separates the phase space into 2 parts, and is a barrier between its interior and its exterior. $\mathfrak{B}$ is given by the deformation $\exp(\{f\})$ of the simple barrier $\mathfrak{B}_0$.

The section of this barrier on the sub space (x, y, t) is topologically equivalent to a torus $\mathbb{T}^2$.

This method of control has been successfully applied to a real machine: a traveling wave tube to reduce its chaos [6].

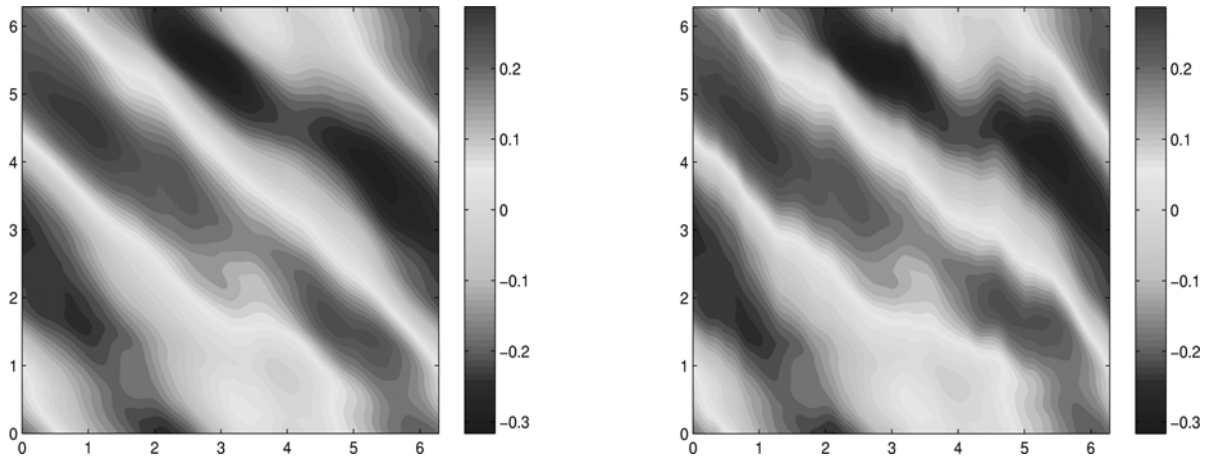

Figure 1: Uncontrolled and controlled potential for $\varepsilon = 0.6$, $t = \frac{\pi}{4}$, $x_0 = 2$

4.2 Properties of the control term

In this Section, we estimate the size and the regularity of the control term (15).

Theorem 2 *For the phenomenological potential (5) the control term (15) verifies:*

$$\|F\|_{\frac{1}{N},\frac{1}{N}} \leq \varepsilon^2 N^2 \frac{e^3}{4\pi} \tag{35}$$

if ε is small enough, i.e. if $|\varepsilon| \leq \frac{\sqrt{\pi}}{2Ne^{3/2}}$ where N is the number of modes in the sum (5).

Proof The proof of this estimation is given in [7] and is based on rewriting

$$\begin{aligned} F = V(x+f') - V(x) &= \int_0^1 ds\ \partial_x V(x+sf', y, \tau) f'(y,\tau) \\ &= \mathcal{O}(V^2) \end{aligned} \tag{36}$$

and then use Cauchy's Theorem.

5 Numerical investigations for the control term

In this Section, we present the results of our numerical investigations for the control term F. The theoretical estimate presented in the previous section shows that its size is quadratic in the perturbation. Figure 1 shows the contour plot of $V(x,y,t)$ and $\widetilde{V}(x,y,t)$ ($\widetilde{V} = V + F$) at some fixed time t, for example $t = \frac{\pi}{4}$. One can see that the contours of both potentials are very similar. But the dynamics of the systems with V and $\tilde{V}$ are very different.

For all numerical simulations we choose the number of modes $N = 25$ in (5). In all plots the abscissa is x and the ordinate is y.

5.1 Phase portrait for the exact control term

To explore the effectiveness of the barrier, we plot (in Fig. 2) the phase portraits for the original system (without control term) and for the system with the exact control term

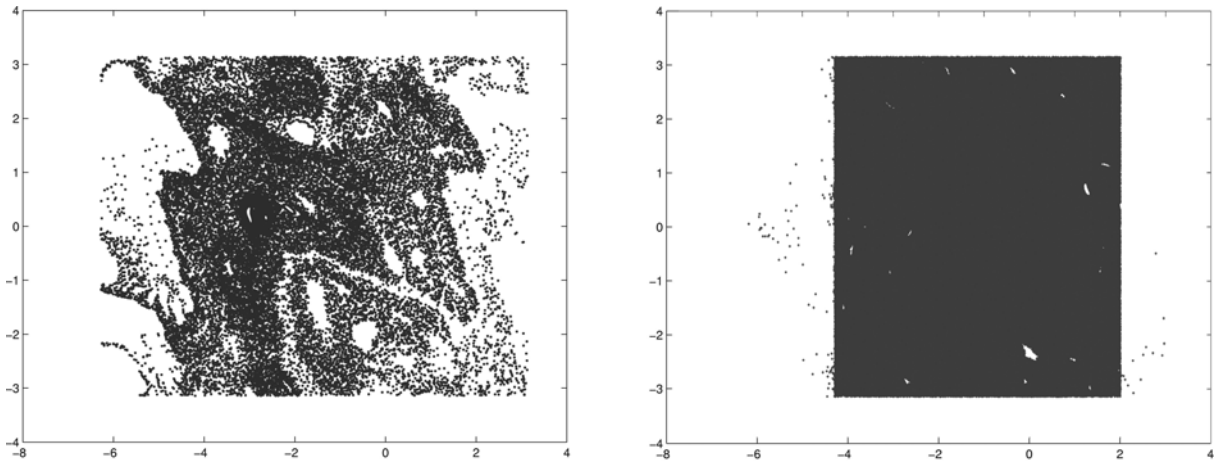

Figure 2: Phase portraits without control term and with the exact control term, for $\varepsilon = 0.9$, $x_0 = 2$, $N_{traj} = 200$

F. We choose the same initial conditions. The time of integration is $T = 2000$, the number of trajectories: $N_{traj} = 200$ (number of initial conditions, all taken in the strip $-1 - \pi \leq x \leq -\pi$; $0 \leq y \leq 2\pi$) and the parameter $\varepsilon = 0.9$. We choose the barrier at position $x_0 = 2$. And to get a Poincaré section, we plot the poloidal section when $t \in 2\pi\mathbb{Z}$. Then we compare the number of trajectories passing through the barrier during this time of integration for each system. We eliminate the points after the crossing. For the uncontrolled system 68% of the initial conditions cross the barrier at $x_0 = 2$ and for the controlled system only 1% of the trajectories escape from the zone of confinement. The theory announces the existence of an exact barrier for the controlled system: these escaped trajectories (1%) are due to numerical errors in the integration.

One can observe that the barrier for the controlled system is a straight line. In fact this barrier moves, its expression depends on time:

$$x = x_0 + f'(y, t) \tag{37}$$

But when $t \in 2\pi\mathbb{Z}$ its oscillation around $x = x_0$ vanishes: $f'(y, 2k\pi) = \int_0^{2k\pi} \partial_y V(x_0, y, t)dt = 0$. This is what we see on this phase portrait. In fact we create 2 barriers at position $x = x_0$, and $x = x_0 - 2\pi$ (and also at $x_0 + 2n\pi$) because of the periodicity of the problem. We note that the mixing increases inside the two barriers. The same phenomenon was also observed in the control of fluids [8], where the same method was applied.

5.2 Robustness of the barrier

In a real Tokamak, it is impossible to know an analytical expression for electric potential V. So we can't implement the exact expression for F. Hence we need to test the robustness of the barrier by truncating the Fourier decomposition (for instance in time) of the controlled potential.

Fourier decomposition

Theorem 3 *The potential (16) can be decomposed as* $\widetilde{V} = \sum_{k\in\mathbb{Z}} \widetilde{V}_k$, *where*

$$\widetilde{V}_k = \varepsilon \sum_{n,m=1}^{N} \frac{\mathcal{J}_k(n\rho)}{(n^2+m^2)^{3/2}} \cos\left(\eta + k\Theta + (k-1)t\right) \tag{38}$$

with

$$\eta_{n,m}(y) = nx + my + \phi_{n,m} + n\varepsilon F_c \tag{39}$$

$$F_c(y) = \sum_{n,m=1}^{N} \frac{m\ \cos(K_{n,m,y})}{(n^2+m^2)^{3/2}} \tag{40}$$

$$F_s(y) = \sum_{n,m=1}^{N} \frac{m\ \sin(K_{n,m,y})}{(n^2+m^2)^{3/2}} \tag{41}$$

$$K_{m,n,y} = nx_0 + my + \phi_{n,m} \tag{42}$$

and $\mathcal{J}_k$ *is the Bessel's function*

$$\mathcal{J}_k(n\rho) = \frac{1}{\pi}\int_0^{\pi} \cos\left(ku - n\rho\sin u\right) du \tag{43}$$

Proof We rewrite explicitly the expression (16) for our phenomenological controlled potential $\widetilde{V}(x,y,t)$:

$$\widetilde{V}(x,y,t) = \varepsilon \sum_{n,m=1}^{N} \frac{\cos\Big(n(x+f'(y,t)) + my + \phi_{n,m} - t\Big)}{(n^2+m^2)^{3/2}} \tag{44}$$

with

$$f'(y,t) = \varepsilon \sum_{n,m=1}^{N} \frac{m\ \Big(\cos K_{n,m,y} - \cos(K_{n,m,y} - t)\Big)}{(n^2+m^2)^{3/2}} \tag{45}$$

With the definition (40) and (41) we have:

$$f'(y,t) = \varepsilon(F_c(y)\ (1-\cos t) - F_s(y)\ \sin t) \tag{46}$$

Let us introduce

$$\rho = \varepsilon(F_c^2 + F_s^2)^{1/2} \tag{47}$$

and Θ by

$$\rho\sin\Theta \equiv -\varepsilon F_c(y) \qquad\qquad \rho\cos\Theta \equiv -\varepsilon F_s(y) \tag{48}$$

so that

$$\widetilde{V} = \varepsilon \sum_{n,m=1}^{N} \frac{\cos\left(\eta - t + n\rho\sin(\Theta + t)\right)}{(n^2+m^2)^{3/2}} \tag{49}$$

Using Bessel's functions properties [9]

$$\cos(\rho\sin\Theta) = \sum_{k\in\mathbb{Z}} \mathcal{J}_k(\rho)\cos k\Theta \tag{50}$$

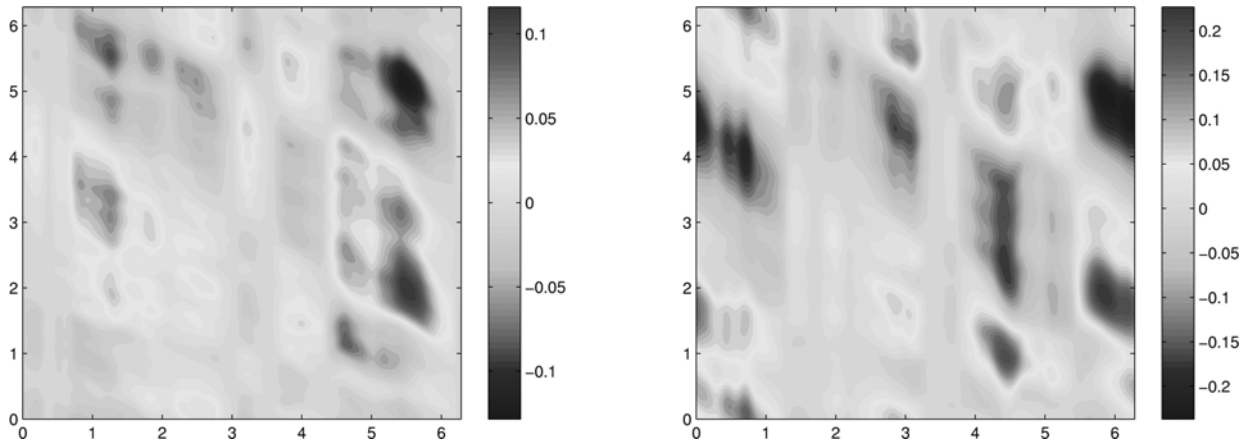

Figure 3: Exact Control Term and Truncated Control Term with $\varepsilon = 0.6, t = \frac{\pi}{4}$

$$\sin(\rho \sin \Theta) = \sum_{k \in \mathbb{Z}} \mathcal{J}_k(\rho) \sin k\Theta \tag{51}$$

we get

$$\cos(\eta - t + n\rho \sin(\Theta + t)) = \sum_{k \in \mathbb{Z}} \mathcal{J}_k(n\rho) \cos(\xi) \tag{52}$$

where $\xi = \eta + k\Theta + (k-1)t$, and we finally obtain (38). The theorem is proved. ■

During numerical simulations we truncate the controlled potential by keeping only its first 3 temporal Fourier's harmonics:

$$\widetilde{V}_{tr} = \varepsilon \sum_{n,m=1}^{N} \frac{A_0 + A_1 \cos t + B_1 \sin t + A_2 \cos 2t + B_2 \sin 2t}{(n^2 + m^2)^{3/2}} \tag{53}$$

$$\begin{aligned}
A_0 &= \mathcal{J}_0(n\rho) \cos(\eta + \Theta) \\
A_1 &= \mathcal{J}_0(n\rho) \cos \eta + \mathcal{J}_2(n\rho) \cos(\eta + 2\Theta) \\
B_1 &= \mathcal{J}_0(n\rho) \sin \eta - \mathcal{J}_2(n\rho) \sin(\eta + 2\Theta) \\
A_2 &= \mathcal{J}_3(n\rho) \cos(\eta + 3\Theta) - \mathcal{J}_1(n\rho) \cos(\eta - \Theta) \\
B_2 &= -\mathcal{J}_3(n\rho) \sin(\eta + 3\Theta) - \mathcal{J}_1(n\rho) \sin(\eta - \Theta)
\end{aligned}$$

Figure 3 compares the two contour plots for the exact control term and the truncated control term (53). Figure4 compares the two phase portraits for the system without control term and for the system with the above truncated control term (53). The computation of $\widetilde{V}_{tr}$ on some grid has been performed in Matlab and the numerical integration of the trajectories was done in C.

One can see a barrier for the system with the truncated control term. As for the system with the exact control term we create two barriers at positions $x = x_0$ and $x = x_0 - 2\pi$ and the phenomenon of increasing the mixing inside the barriers persist.

5.3 Energetical cost

As we have seen before, the introduction of the control term into the system can reduce and even stop the diffusion of the particles through the barrier. Now we estimate the energy cost of the control term F and the truncated control term $F_{tr} \equiv \widetilde{V}_{tr} - V$.

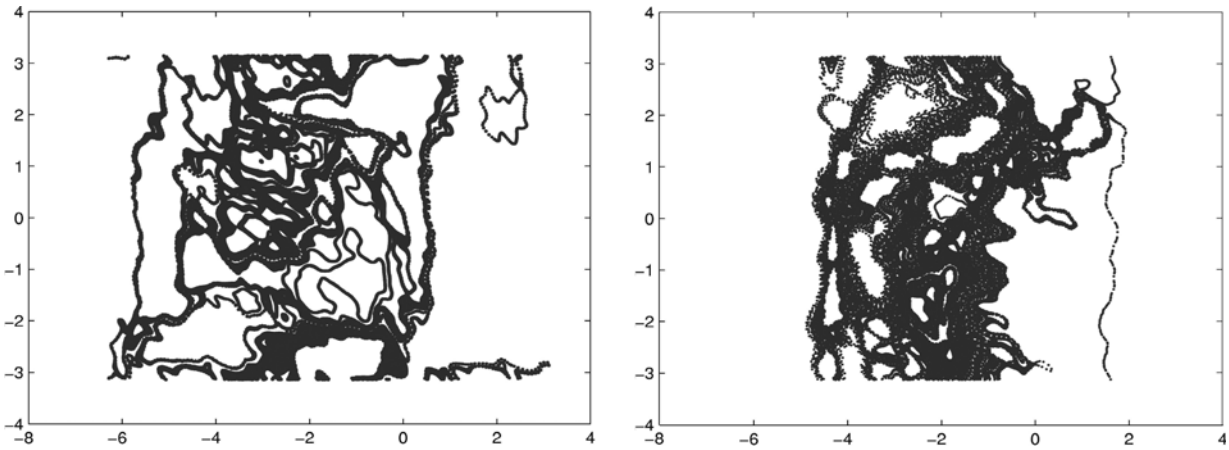

Figure 4: $\varepsilon = 0.3$, $T = 2000$, $N_{traj} = 50$

Table 1: Squared ratios of the amplitudes of the control term and the uncontrolled electric potential ζ_{ex}, ζ_{tr}; ratios of electric energy of the control term and the uncontrolled electic potential η_{ex}, η_{tr}; for the system with exact and truncated control term.

ε	ζ_{ex}	ζ_{tr}	η_{ex}	η_{tr}
0.3	0.1105	0.1193	0.6297	0.1431
0.4	0.1466	0.1583	0.7145	0.2393
0.5	0.1822	0.1967	0.8161	0.3550
0.6	0.2345	0.2137	0.9336	0.4883
0.7	0.2518	0.2716	1.0657	0.6375
0.8	0.2858	0.3038	1.2119	0.8014
0.9	0.3191	0.3439	1.3722	0.9796
1.5	0.5052	0.5427	2.6247	2.3037

The average of any function $W = W(x, y, \tau)$ is defined by the formula:

$$< |W| >= \int_0^{2\pi} dx \int_0^{2\pi} dy \int_0^{2\pi} dt \; |W(x, y, t)| \tag{54}$$

Now we calculate the ratio between the absolute value of the truncated control (electric potential) or the exact control and the uncontrolled electric potential:

$$\zeta_{ex} =< |F|^2 > / < |V|^2 >$$

and

$$\zeta_{tr} =< |F_{tr}|^2 > / < |V|^2 >$$

We also compute the ratio between the energy of the control electric field and the energy of the uncontrolled system in their exact and truncated version

$$\eta_{ex} =< |\nabla F|^2 > / < |\nabla V|^2 >$$

and

$$\eta_{tr} =< |\nabla F_{tr}|^2 > / < |\nabla V|^2 >$$

for different values of ε. Results are shown in Table 1.

Table 2: Number of escaping particles without control term $\mathcal{N}_{without}$, and for the system with the exact control term $\mathcal{N}_{exact}$ and the truncated control term $\mathcal{N}_{tr}$.

ε	$\mathcal{N}_{without}$	$\mathcal{N}_{exact}$	$\mathcal{N}_{tr}$
0.4	22%	0%	6%
0.5	26%	0%	18%
0.9	68%	1%	44%
1.5	72%	1%	54%

Table 3: Difference $\Delta\mathcal{N}$ of the number of particles passing trough the barrier and difference of relative electric energy $\Delta\eta$ for the controlled and uncontrolled system.

ε	$\Delta\mathcal{N}$	$\Delta\eta$
0.3	8%	0.49
0.4	16%	0.47
0.5	8%	0.46
0.9	24%	0.39
1.5	18%	0.32

One can see that the truncated control term needs a smaller energy than the exact control term. In Table 2, we present the number of particles passing through the barrier in function of ε, after the same integration time.

Let $\Delta\mathcal{N} = \mathcal{N}_{without} - \mathcal{N}_{tr}$ be the difference between the number of particles passing through the barrier for the system without control and with the truncated control and $\Delta\eta = \eta_{ex} - \eta_{tr}$ the difference between the relative electric energy for the system with the exact control term and the system with the truncated control term. In Table 3 we present $\Delta\mathcal{N}$ and $\Delta\eta$ for differents values of ε.

For ε below 0.2 the non controlled system is rather regular, there is no particles stream through the barrier, so we have no need to introduce the control electric field. For ε between 0.3 and 0.9 the truncated control field is quite efficient, it allows to drop the chaotic transport through the barrier by a factor 8% to 24% with respect to the uncontrolled system and it requires less energy than the exact control field. For ε greater than 1 the truncated control field is less efficient than the exact one, because the dynamics of the system is very chaotic. For example when $\varepsilon = 1.5$, there are 72% of the particles crossing the barrier for the uncontrolled system and 54% for the system with the truncated control field. At the same time the energetical cost of the truncated control field is above 70% of the exact one, which allows to stop the transport through the barrier. So for $\varepsilon \geq 1$ we need to use the exact control field rather than the truncated one.

6 Discussion and Conclusion

In this article, we studied a possible improvement of the confinement properties of a magnetized fusion plasma. A transport barrier conception method is proposed as an alternative to presently achieved barriers such as the H-mode and the ITB scenarios. One can remark, that our method differs from an ITB construction. Indeed, in order to build-up a transport barrier, we do not require a hard modification of the system, such as a change in the q-profile. Rather, we propose a weak change of the system properties that allow a barrier to develop. However, our control scheme requires some knowledge and information relative to the turbulence at work, these having weak or no impact on the

ITB scenarios.

6.1 Main results

First of all we have proved that the local control theory gives the possibility to construct a transport barrier at any chosen position $x = x_0$ for any electric potential $V(x, y, t)$. Indeed, the proof given in section 4 does not depend on the model for the electric potential V. In Subsection 4.1, we give a rigorous estimate for the norm of the control term F, for some phenomenological model of the electric potential. The introduction of the exact control term into the system inhibits the particle transport through the barrier for any ε while the implementation of a truncated control term reduces the particle transport significantly for $\varepsilon \in (0.3, 1.0)$.

6.2 Discussion, open questions

6.2.1 Comparison with the global control method

Let us now compare our approach with the global control method [3] which aims at globally reducing the transport in every point of the phase space. Our approach aims at implementing a transport barrier. However, one also observes a global modification of the dynamics since the mixing properties seem to increase away from the barriers.

Furthermore, in many cases, only the first few terms of the expansion of the global control term [3] can be computed explicitly. Here we have an explicit exact expression for the local control term.

6.2.2 Implementation of the control procedure

Let us now consider the implementation of our method to turbulent plasmas where the turbulent electric field is consistent with the particle transport. The theoretical proof of an hamiltonian control concept is developped provided the system properties at work are completely known. For example the analytic expression for the electric potential. This is impossible in a real system, since the measurements take place on a finite spatio-temporal grid. This has motivated our investigation of the truncated control term by reducing the actually used information on the system. As pointed out previously, one finds that this approach is ineffective for strong turbulence. Another issue is the evolution of the turbulent electric field following the appearance of a transport barrier. This issue would deserve a specific analysis and very likely updating the control term on a trasnport characteristic time scale. An alternative to such a process would be to use a retroactive Hamiltonian approach (a classical field theory) [10] and to develop the control theory in that framework.

Acknowledgements

We acknowledge very useful and encouraging discussions with Ph. Ghendrih, A. Brizard, C. Chandre, G. Ciraolo and M. Pettini. This work supported by the European Communities under the contract of Association between EURATOM and CEA was carried out within the framework of the European Fusion Development Agreement. The views and opinions expressed herein do not necessarily reflect those of the European Commission.

References

[1] F. Wagner and U. Stroth, Plasma Phys. Contr. Fusion, **35**, 1321 (1993).

[2] E.J. Doyle et al., Nucl. Fus.,**47** S18 (2007).

[3] G. Ciraolo, F. Briolle, C. Chandre, E. Floriani, R. Lima, M. Vittot, M. Pettini, Ch. Figarella, Ph. Ghendrih: "Control of Hamiltonian chaos as a possible tool to control anomalous transport in fusion plasmas", Phys. Rev. E, **69**, 056213 (2004).

[4] J. Wesson, *Tokamaks*, Oxford University Press (2004).

[5] M. Pettini, A. Vulpiani, J. H. Misguich, M. De Leener, J. Orban, R. Balescu: "Chaotic diffusion across a magnetic field in a model of electrostatic turbulent plasma", Phys. Rev. A **38**, (1988) p 344-363.

[6] C. Chandre, G. Ciarolo, F. Doveil, R. Lima, A. Macor, M. Vittot: "Channelling chaos by building barriers", Phys. Rev. Lett. **94**, 074101 (2005).

[7] N. Tronko, M. Vittot: "Localized control theory for hamiltonian systems and its application to the chaotic transport of test particules in plasmas". To appear in the proceedings of the "Joint Varenna - Lausanne International Workshop: Theory of Fusion Plasmas", Varenna (August 2008)

[8] T. Benzekri, C. Chandre, X. Leoncini, R. Lima, M. Vittot: "Chaotic advection and targeted mixing", Phys. Rev. Lett. **96**, 124503 (2006).

[9] M. Abramowitz, I. A. Stegun, eds. *Handbook of Mathematical Functions*, (Dover, New York, 1965), p 361.

[10] I. Bialynicki-Birula, J. C. Hubbard, L. A. Turski: "Gauge-independent canonical formulation of relativistic plasma theory", Physica A **128** (1984) p 509-519.